

Bayesian signal reconstruction for 1-bit compressed sensing

Yingying Xu¹, Yoshiyuki Kabashima¹ and Lenka Zdeborová²

¹Department of Computational Intelligence and Systems Science,
Tokyo Institute of Technology, Yokohama 226-8502, Japan

²Institut de Physique Théorique, IPhT, CEA Saclay, and URA 2306, CNRS,
F-91191 Gif-sur-Yvette, France

E-mail: yingxu@sp.dis.titech.ac.jp, kaba@dis.titech.ac.jp,
lenka.zdeborova@cea.fr

Abstract. The 1-bit compressed sensing framework enables the recovery of a sparse vector \mathbf{x} from the sign information of each entry of its linear transformation. Discarding the amplitude information can significantly reduce the amount of data, which is highly beneficial in practical applications. In this paper, we present a Bayesian approach to signal reconstruction for 1-bit compressed sensing, and analyze its typical performance using statistical mechanics. As a basic setup, we consider the case that the measuring matrix Φ has i.i.d entries, and the measurements \mathbf{y} are noiseless. Utilizing the replica method, we show that the Bayesian approach enables better reconstruction than the l_1 -norm minimization approach, asymptotically saturating the performance obtained when the non-zero entries positions of the signal are known, for signals whose non-zero entries follow zero mean Gaussian distributions. We also test a message passing algorithm for signal reconstruction on the basis of belief propagation. The results of numerical experiments are consistent with those of the theoretical analysis.

1. Introduction

Compressed (or compressive) sensing (CS) is currently one of the most popular topics in information science, and has been used for applications in various engineering fields, such as audio and visual electronics, medical imaging devices, and astronomical observations [1]. Typically, smooth signals, such as natural images and communications signals, can be represented by a sparsity-inducing basis, such as a Fourier or wavelet basis [2, 3]. The goal of CS is to reconstruct a high-dimensional signal from its lower-dimensional linear transformation data, utilizing the prior knowledge on the sparsity of the signal [4]. This results in time, cost, and precision advantages.

Mathematically, the CS problem can be expressed as follows: an N -dimensional vector \mathbf{x}^0 is linearly transformed into an M -dimensional vector \mathbf{y} by an $M \times N$ -dimensional measurement matrix Φ , as $\mathbf{y} = \Phi \mathbf{x}^0$ [4]. The observer is free to choose the measurement protocol. Given Φ and \mathbf{y} , the central problem is how to reconstruct \mathbf{x}^0 . When $M < N$, due to the loss of information, the inverse problem has infinitely many solutions. However, when it is guaranteed that \mathbf{x}^0 has only $K < M$ nonzero entries in some convenient basis (i.e., when the signal is sparse enough) and the measurement matrix is incoherent with that basis, there is a high probability that the inverse problem has a unique and exact solution. Considerable efforts have been made to clarify the condition for the uniqueness and correctness of the solution, and to develop practically feasible signal reconstruction algorithms [5, 6, 7, 8, 9].

Recently, a scheme called *1-bit compressed sensing (1-bit CS)* was proposed. In 1-bit CS, the signal is recovered from only the sign data of the linear measurements $\mathbf{y} = \text{sign}(\Phi \mathbf{x}^0)$, where $\text{sign}(x) = x/|x|$ for $x \neq 0$ is a component-wise operation when x is a vector [10]. Discarding the amplitude information can significantly reduce the amount of data to be stored and/or transmitted. This is highly advantageous for most real-world applications, particularly those in which the measurement is accompanied by the transmission of digital information [11]. In 1-bit CS, the amplitude information is lost during the measurement stage, making perfect recovery of the original signal impossible. Thus, we generally need more measurements to compensate for the loss of information. The scheme is considered to have practical relevance in situations where perfect recovery is not required, and measurements are inexpensive but precise quantization is expensive. These features are very different from those of general CS.

The most widely used signal reconstruction scheme in CS is l_1 -norm minimization, which searches for the vector with the smallest l_1 -norm $\|\mathbf{x}\|_1 = \sum_{i=1}^N |x_i|$ under the constraint $\mathbf{y} = \Phi \mathbf{x}$. This is based on the work of Candès et al. [4]–[6], who also suggested the use of a random measurement matrix Φ with independent and identically distributed entries. Because the optimization problem is convex and can be solved using efficient linear programming techniques, these ideas have led to various fast and efficient algorithms. The l_1 -reconstruction is now widely used, and is responsible for the surge of interest in CS over the past few years. Against this background, l_1 -reconstruction was the first technique attempted in the development of the 1-bit CS problem. In [10],

an approximate signal recovery algorithm was proposed based on the minimization of the l_1 -norm under the constraint $\text{sign}(\Phi \mathbf{x}) = \mathbf{y}$, and its utility was demonstrated by numerical experiments. In [12], the capabilities of this method were analyzed, and a new algorithm based on the cavity method was presented. However, the significance of the l_1 -based scheme may be rather weak for 1-bit CS, because the loss of convexity prevents the development of mathematically guaranteed and practically feasible algorithms.

Therefore, we propose another approach based on Bayesian inference for 1-bit CS, focused on the case that each entry of Φ is independently generated from a standard Gaussian distribution, and the output \mathbf{y} is noiseless. Although the Bayesian approach is guaranteed to achieve the optimal performance when the actual signal distribution is given, quantifying the performance gain is a nontrivial task. We accomplish this task utilizing the replica method, which shows that when non-zero entries of the signal follow zero mean Gaussian distributions, the Bayesian optimal inference asymptotically saturates the mean squared error (MSE) performance obtained when the positions of non-zero signal entries are known as $\alpha = M/N \rightarrow \infty$. This means that, in such cases, at least in terms of MSEs, the correct prior knowledge of the sparsity asymptotically becomes as informative as the knowledge of the exact positions of the non-zero entries. Unfortunately, performing the exact Bayesian inference is computationally difficult. This difficulty is resolved by employing the generalized approximate message passing technique, which is regarded as a variation of belief propagation or the cavity method [13, 14].

This paper is organized as follows. The next section sets up the 1-bit CS problem. In section 3, we examine the signal recovery performance achieved by the Bayesian scheme utilizing the replica method. In section 4, an approximate signal recovery algorithm based on belief propagation is developed. The utility of this algorithm is tested and its asymptotic performance is analyzed in section 5. The final section summarizes our work.

2. Problem setup and Bayesian optimality

Let us suppose that entry x_i^0 ($i = 1, 2, \dots, N$) of an N -dimensional signal (vector) $\mathbf{x}^0 = (x_i^0) \in \mathbb{R}^N$ is independently generated from an identical sparse distribution:

$$P(x) = (1 - \rho) \delta(x) + \rho \tilde{P}(x), \quad (1)$$

where $\rho \in [0, 1]$ represents the density of nonzero entries in the signal, and $\tilde{P}(x)$ is a distribution function of $x \in \mathbb{R}$ that has a finite second moment and does not have finite mass at $x = 0$. In 1-bit CS, the measurement is performed as

$$\mathbf{y} = \text{sign}(\Phi \mathbf{x}^0), \quad (2)$$

where $\text{sign}(x) = x/|x|$ operates in a component-wise manner, and for simplicity we assume that each entry of the $M \times N$ measurement matrix Φ is provided as a sample of a Gaussian distribution of zero mean and variance N^{-1} .

We shall adopt the Bayesian approach to reconstruct the signal from the 1-bit measurement \mathbf{y} assuming that Φ is correctly known in the recovery stage. Let us denote an arbitrary recovery scheme for the measurement \mathbf{y} as $\hat{\mathbf{x}}(\mathbf{y})$, where we impose a normalization constraint $|\hat{\mathbf{x}}(\mathbf{y})|^2 = N\rho$ to compensate for the loss of amplitude information by the 1-bit measurement. Equations (1) and (2) indicate that, for a given Φ , the joint distribution of the sparse vector and its 1-bit measurement is

$$P(\mathbf{x}, \mathbf{y} | \Phi) = \prod_{\mu=1}^M \Theta(y_{\mu}(\Phi \mathbf{x})_{\mu}) \times \prod_{i=1}^N \left((1 - \rho) \delta(x_i) + \rho \tilde{P}(x_i) \right), \quad (3)$$

where $\Theta(x) = 1$ for $x > 0$, and vanishes otherwise. This generally provides $\hat{\mathbf{x}}(\cdot)$ with the mean square error, which is hereafter handled as the performance measure for the signal reconstruction[‡], as follows:

$$\text{MSE}(\hat{\mathbf{x}}(\cdot)) = \sum_{\mathbf{y}} \int d\mathbf{x} P(\mathbf{x}, \mathbf{y} | \Phi) \left| \frac{\hat{\mathbf{x}}(\mathbf{y})}{|\hat{\mathbf{x}}(\mathbf{y})|} - \frac{\mathbf{x}}{|\mathbf{x}|} \right|^2. \quad (4)$$

The following theorem forms the basis of our Bayesian approach.

Theorem 1. $\text{MSE}(\hat{\mathbf{x}}(\cdot))$ is lower bounded as

$$\text{MSE}(\hat{\mathbf{x}}(\cdot)) \geq 2 \sum_{\mathbf{y}} P(\mathbf{y} | \Phi) \left(1 - \left| \left\langle \frac{\mathbf{x}}{|\mathbf{x}|} \right\rangle_{|\mathbf{y}, \Phi} \right| \right), \quad (5)$$

where

$$\begin{aligned} P(\mathbf{y} | \Phi) &= \int d\mathbf{x} P(\mathbf{x}, \mathbf{y} | \Phi) \\ &= \int d\mathbf{x} \prod_{\mu=1}^M \Theta(y_{\mu}(\Phi \mathbf{x})_{\mu}) \times \prod_{i=1}^N \left((1 - \rho) \delta(x_i) + \rho \tilde{P}(x_i) \right) \end{aligned} \quad (6)$$

is the marginal distribution of the 1-bit measurement \mathbf{y} and $\langle f(\mathbf{x}) \rangle_{|\mathbf{y}, \Phi} = \int d\mathbf{x} f(\mathbf{x}) P(\mathbf{x} | \mathbf{y}, \Phi) = \int d\mathbf{x} f(\mathbf{x}) P(\mathbf{x}, \mathbf{y} | \Phi) / P(\mathbf{y} | \Phi)$ generally denotes the posterior mean of an arbitrary function of \mathbf{x} , $f(\mathbf{x})$, given \mathbf{y} . The equality holds for the Bayesian optimal signal reconstruction

$$\hat{\mathbf{x}}^{\text{Bayes}}(\mathbf{y}) = \sqrt{N\rho} \left| \left\langle \frac{\mathbf{x}}{|\mathbf{x}|} \right\rangle_{|\mathbf{y}, \Phi} \right|^{-1} \left\langle \frac{\mathbf{x}}{|\mathbf{x}|} \right\rangle_{|\mathbf{y}, \Phi}. \quad (7)$$

Proof. Employing the Bayes formula $P(\mathbf{x}, \mathbf{y} | \Phi) = P(\mathbf{x} | \mathbf{y}, \Phi) P(\mathbf{y} | \Phi)$ in (4) yields the expression

$$\begin{aligned} \text{MSE}(\hat{\mathbf{x}}(\cdot)) &= \sum_{\mathbf{y}} \int d\mathbf{x} P(\mathbf{x}, \mathbf{y} | \Phi) \left| \frac{\hat{\mathbf{x}}(\mathbf{y})}{|\hat{\mathbf{x}}(\mathbf{y})|} - \frac{\mathbf{x}}{|\mathbf{x}|} \right|^2 \\ &= \sum_{\mathbf{y}} \int d\mathbf{x} P(\mathbf{x} | \mathbf{y}, \Phi) P(\mathbf{y} | \Phi) \left(\left| \frac{\hat{\mathbf{x}}(\mathbf{y})}{|\hat{\mathbf{x}}(\mathbf{y})|} \right|^2 + \left| \frac{\mathbf{x}}{|\mathbf{x}|} \right|^2 - 2 \frac{\hat{\mathbf{x}}(\mathbf{y}) \cdot \mathbf{x}}{|\hat{\mathbf{x}}(\mathbf{y})| |\mathbf{x}|} \right) \end{aligned}$$

[‡] Errors of other types, such as l_p -norm, can also be chosen as the performance measure. The argument shown in this section holds similarly even when such measures are used.

$$= 2 \sum_{\mathbf{y}} P(\mathbf{y}|\Phi) \left(1 - \frac{\hat{\mathbf{x}}(\mathbf{y})}{|\hat{\mathbf{x}}(\mathbf{y})|} \cdot \left\langle \frac{\mathbf{x}}{|\mathbf{x}|} \right\rangle_{|\mathbf{y}, \Phi} \right). \quad (8)$$

Inserting the Cauchy–Schwarz inequality

$$\hat{\mathbf{x}}(\mathbf{y}) \cdot \left\langle \frac{\mathbf{x}}{|\mathbf{x}|} \right\rangle_{|\mathbf{y}, \Phi} \leq |\hat{\mathbf{x}}(\mathbf{y})| \left| \left\langle \frac{\mathbf{x}}{|\mathbf{x}|} \right\rangle_{|\mathbf{y}, \Phi} \right| \quad (9)$$

into the right-hand side of (8) yields the lower bound of (5), where the equality holds when $\hat{\mathbf{x}}(\mathbf{y})$ is parallel to $\left\langle \frac{\mathbf{x}}{|\mathbf{x}|} \right\rangle_{|\mathbf{y}, \Phi}$. This, in conjunction with the normalization constraint of $\hat{\mathbf{x}}(\mathbf{y})$, leads to (7). \square

The above theorem guarantees that the Bayesian approach achieves the best possible performance in terms of MSE. Therefore, we hereafter focus on the reconstruction scheme of (7), quantitatively evaluate its performance, and develop a computationally feasible approximate algorithm.

3. Performance assessment by the replica method

In statistical mechanics, the macroscopic behavior of the system is generally analyzed by evaluating the partition function or its negative logarithm, free energy. In our signal reconstruction problem, the marginal likelihood $P(\mathbf{y}|\Phi)$ of (6) plays the role of the partition function. However, this still depends on the quenched random variables \mathbf{y} and Φ . Therefore, we must further average the free energy as $\bar{f} \equiv -N^{-1} [\log P(\mathbf{y}|\Phi)]_{\mathbf{y}, \Phi}$ to evaluate the typical performance, where $[\cdots]_{\mathbf{y}, \Phi}$ denotes the configurational average concerning \mathbf{y} and Φ .

Unfortunately, directly averaging the logarithm of random variables is, in general, technically difficult. Thus, we resort to the replica method to practically resolve this difficulty [15]. For this, we first evaluate the n -th moment of the marginal likelihood $[P^n(\mathbf{y}|\Phi)]_{\Phi, \mathbf{y}}$ for $n = 1, 2, \dots \in \mathbb{N}$ using the formula

$$P^n(\mathbf{y}|\Phi) = \int \prod_{a=1}^n (d\mathbf{x}^a P(\mathbf{x}^a)) \prod_{a=1}^n \prod_{\mu=1}^M \Theta((\mathbf{y})_{\mu}(\Phi \mathbf{x}^a)_{\mu}), \quad (10)$$

which holds only for $n = 1, 2, \dots \in \mathbb{N}$. Here, \mathbf{x}^a ($a = 1, 2, \dots, n$) denotes the a -th replicated signal. Averaging (10) with respect to Φ and \mathbf{y} results in the saddle-point evaluation concerning the macroscopic variables $q_{0a} = q_{a0} \equiv N^{-1} \mathbf{x}^0 \cdot \mathbf{x}^a$ and $q_{ab} = q_{ba} \equiv N^{-1} \mathbf{x}^a \cdot \mathbf{x}^b$ ($a, b = 1, 2, \dots, n$).

Although (10) holds only for $n \in \mathbb{N}$, the expression $N^{-1} \log [P^n(\mathbf{y}|\Phi)]_{\Phi, \mathbf{y}}$ obtained by the saddle-point evaluation under a certain assumption concerning the permutation symmetry with respect to the replica indices $a, b = 1, 2, \dots, n$ is obtained as an analytic function of n , which is likely to also hold for $n \in \mathbb{R}$. Therefore, we next utilize the analytic function to evaluate the average of the logarithm of the partition function as

$$\bar{f} = - \lim_{n \rightarrow 0} (\partial / \partial n) N^{-1} \log [P^n(\mathbf{y}|\Phi)]_{\mathbf{y}, \Phi}. \quad (11)$$

In particular, under the replica symmetric ansatz, where the dominant saddle-point is assumed to be of the form

$$q_{ab} = q_{ba} = \begin{cases} \rho & (a = b = 0) \\ m & (a = 1, 2, \dots, n; b = 0) \\ Q & (a = b = 1, 2, \dots, n) \\ q & (a \neq b = 1, 2, \dots, n) \end{cases}, \quad (12)$$

The above procedure expresses the average free energy density as

$$\begin{aligned} \bar{f} = -\text{extr}_{\omega} & \left\{ \int dx^0 P(x^0) \int Dz \phi(\sqrt{\hat{q}}z + \hat{m}x^0; \hat{Q}) + \frac{1}{2}Q\hat{Q} + \frac{1}{2}q\hat{q} - m\hat{m} \right. \\ & \left. + 2\alpha \int Dt H\left(\frac{m}{\sqrt{\rho q - m^2}}t\right) \log H\left(\sqrt{\frac{q}{Q - q}}t\right) \right\}. \end{aligned} \quad (13)$$

Here, $\alpha = M/N$, $H(x) = \int_x^{+\infty} Dz$, $Dz = dz \exp(-z^2/2)/\sqrt{2\pi}$ is a Gaussian measure, $\text{extr}_X\{g(X)\}$ denotes the extremization of a function $g(X)$ with respect to X , $\omega = \{Q, q, m, \hat{Q}, \hat{q}, \hat{m}\}$, and

$$\begin{aligned} & \phi(\sqrt{\hat{q}}z + \hat{m}x^0; \hat{Q}) \\ & = \log \left\{ \int dx P(x) \exp\left(-\frac{\hat{Q} + \hat{q}}{2}x^2 + (\sqrt{\hat{q}}z + \hat{m}x^0)x\right) \right\}. \end{aligned} \quad (14)$$

The derivation of (13) is provided in Appendix A.

In evaluating the right-hand side of (11), $P(\mathbf{y}|\Phi)$ not only gives the marginal likelihood (the partition function), but also the conditional density of \mathbf{y} for taking the configurational average. This accordance between the partition function and the distribution of the quenched random variables is generally known as the Nishimori condition in spin glass theory [16], for which the replica symmetric ansatz (12) is supported by other schemes than the replica method [17, 18], yielding the identity $[P^n(\mathbf{y}|\Phi)]_{\mathbf{y}, \Phi} = \int d\Phi P(\Phi) \left(\sum_{\mathbf{y}} P^{n+1}(\mathbf{y}|\Phi)\right)$. This indicates that the true signal, \mathbf{x}^0 , can be handled on an equal footing with the other n replicated signals $\mathbf{x}^1, \mathbf{x}^2, \dots, \mathbf{x}^n$ in the replica computation. As $n \rightarrow 0$, this higher replica symmetry among the $n+1$ replicated variables allows us to further simplify the replica symmetric ansatz (12) by imposing four extra constraints: $Q = \rho$, $q = m$, $\hat{Q} = 0$, and $\hat{q} = \hat{m}$. As a consequence, the extremization condition of (13) is summarized by the non-linear equations

$$m = \int Dt \frac{\left(\int dx x e^{-\frac{\hat{m}}{2}x^2 + \sqrt{\hat{m}}tx} P(x)\right)^2}{\int dx e^{-\frac{\hat{m}}{2}x^2 + \sqrt{\hat{m}}tx} P(x)} \quad (15)$$

$$\hat{m} = \frac{\alpha}{\pi\sqrt{2\pi}(\rho - m)} \int dt \frac{\exp\left\{-\frac{\rho+m}{2(\rho-m)}t^2\right\}}{H\left(\sqrt{\frac{m}{\rho-m}}t\right)}. \quad (16)$$

In physical terms, the value of m determined by these equations is the typical overlap $N^{-1}[\mathbf{x}^0 \cdot \langle \mathbf{x} \rangle_{\mathbf{y}, \Phi}]_{\mathbf{y}, \Phi}$ between the original signal \mathbf{x}^0 and the posterior mean

$\langle \mathbf{x} \rangle_{\mathbf{y}, \Phi}$. The law of large numbers and the self-averaging property guarantee that both $N^{-1}|\mathbf{x}|^2$ and $N^{-1}|\mathbf{x}^0|^2$ converge to ρ with a probability of unity for typical samples. This indicates that the typical value of the direction cosine between \mathbf{x}^0 and $\hat{\mathbf{x}}^{\text{Bayes}}(\mathbf{y})$ can be evaluated as $[(\mathbf{x}^0 \cdot \hat{\mathbf{x}}^{\text{Bayes}}(\mathbf{y})) / (|\mathbf{x}^0| |\hat{\mathbf{x}}^{\text{Bayes}}(\mathbf{y})|)]_{\mathbf{y}, \Phi} \simeq [(\mathbf{x}^0 \cdot \langle \mathbf{x} \rangle_{\mathbf{y}, \Phi})]_{\mathbf{y}, \Phi} / \left([|\mathbf{x}^0|]_{\mathbf{x}^0} [|\langle \mathbf{x} \rangle_{\mathbf{y}, \Phi}|]_{\mathbf{y}, \Phi} \right) = Nm / (N\sqrt{\rho m}) = \sqrt{m/\rho}$. Therefore, the MSE in (4) can be expressed using m and ρ as

$$\text{MSE} = 2 \left(1 - \sqrt{\frac{m}{\rho}} \right). \quad (17)$$

The symmetry between \mathbf{x}^0 and the other replicated variables \mathbf{x}^a ($a = 1, 2, \dots, n$) provides \bar{f} with further information-theoretic meanings. Inserting $P(\mathbf{y}, \Phi) = P(\mathbf{y}|\Phi)P(\Phi)$ into the definition of \bar{f} gives $\bar{f} = N^{-1} \int d\Phi P(\Phi) \left(-\sum_{\mathbf{y}} P(\mathbf{y}|\Phi) \log P(\mathbf{y}|\Phi) \right)$, which indicates that \bar{f} accords with the entropy density of \mathbf{y} for typical measurement matrices Φ . The expression $P(\mathbf{y}|\mathbf{x}, \Phi) = \prod_{\mu=1}^M \Theta(y_{\mu}(\Phi\mathbf{x})_{\mu}) \in \{0, 1\}$ guarantees that the conditional entropy of \mathbf{y} given \mathbf{x} and Φ , $-\sum_{\mathbf{y}} P(\mathbf{y}|\mathbf{x}, \Phi) \log P(\mathbf{y}|\mathbf{x}, \Phi)$, always vanishes. These indicate that \bar{f} also implies a mutual information density between \mathbf{y} and \mathbf{x} . This physically quantifies the optimal information gain (per entry) of \mathbf{x} that can be extracted from the 1-bit measurement \mathbf{y} for typical Φ .

4. Bayesian optimal signal reconstruction by GAMP

Equation (17) represents the potential performance of the Bayesian optimal signal reconstruction of 1-bit CS. However, in practice, exploiting this performance is a non-trivial task, because performing the exact Bayesian reconstruction (7) is computationally difficult. To resolve this difficulty, we now develop an approximate reconstruction algorithm following the framework of belief propagation (BP). Actually, BP has been successfully employed for standard CS problems with linear measurements, showing excellent performance in terms of both reconstruction accuracy and computational efficiency [19]. To incorporate the non-linearity of the 1-bit measurement, we employ a variant of BP known as generalized approximate message passing (GAMP) [13], which can also be regarded as an approximate Bayesian inference algorithm for perceptron-type networks [14].

In general, the canonical BP equations for the probability measure $P(\mathbf{x}|\Phi, \mathbf{y})$ are expressed in terms of $2MN$ messages, $m_{i \rightarrow \mu}(x_i)$ and $m_{\mu \rightarrow i}(x_i)$ ($i = 1, 2, \dots, N; \mu = 1, 2, \dots, M$), which represent probability distribution functions that carry posterior information and output measurement information, respectively. They can be written as

$$m_{\mu \rightarrow i}(x_i) = \frac{1}{Z_{\mu \rightarrow i}} \int \prod_{j \neq i} dx_j P(y_{\mu} | u_{\mu}) \prod_{j \neq i} m_{j \rightarrow \mu}(x_j) \quad (18)$$

$$m_{i \rightarrow \mu}(x_i) = \frac{1}{Z_{i \rightarrow \mu}} P(x_i) \prod_{\gamma \neq \mu} m_{\gamma \rightarrow i}(x_i) \quad (19)$$

Here, $Z_{\mu \rightarrow i}$ and $Z_{i \rightarrow \mu}$ are normalization factors ensuring that $\int dx_i m_{\mu \rightarrow i}(x_i) = \int dx_i m_{i \rightarrow \mu}(x_i) = 1$, and we also define $u_\mu \equiv (\Phi \mathbf{x})_\mu$. Using (18), the approximation of marginal distributions $P(x_i | \Phi, \mathbf{y}) = \int \prod_{j \neq i} dx_j P(\mathbf{x} | \Phi, \mathbf{y})$, which are often termed beliefs, are evaluated as

$$m_i(x_i) = \frac{1}{Z_i} P(x_i) \prod_{\mu=1}^M m_{\mu \rightarrow i}(x_i), \quad (20)$$

where Z_i is a normalization factor for $\int dx_i m_i(x_i) = 1$. To simplify the notation, we hereafter convert all measurement results to +1 by multiplying each row of the measurement matrix $\Phi = (\Phi_{\mu i})$ by y_μ ($\mu = 1, 2, \dots, N$), giving $(\Phi_{\mu i}) \rightarrow (y_\mu \Phi_{\mu i})$, and denote the resultant matrix as $\Phi = (\Phi_{\mu i})$. In the new notation, $P(y_\mu | u_\mu) = \Theta(u_\mu)$.

Next, we introduce means and variances of x_i in the posterior information message distributions as

$$a_{i \rightarrow \mu} \equiv \int dx_i x_i m_{i \rightarrow \mu}(x_i) \quad (21)$$

$$\nu_{i \rightarrow \mu} \equiv \int dx_i x_i^2 m_{i \rightarrow \mu}(x_i) - a_{i \rightarrow \mu}^2. \quad (22)$$

We also define $\omega_\mu \equiv \sum_i \Phi_{\mu i} a_{i \rightarrow \mu}$ and $V_\mu \equiv \sum_i \Phi_{\mu i}^2 \nu_{i \rightarrow \mu}$ for notational convenience. Similarly, the means and variances of the beliefs, a_i and ν_i , are introduced as $a_i \equiv \int dx_i x_i m_i(x_i)$ and $\nu_i \equiv \int dx_i x_i^2 m_i(x_i) - a_i^2$. Note that $\mathbf{a} = (a_i)$ represents the approximation of the posterior mean $\langle \mathbf{x} \rangle_{|\mathbf{y}, \Phi}$. This, in conjunction with a consequence of the law of large numbers $\langle \mathbf{x} / |\mathbf{x}| \rangle_{|\mathbf{y}, \Phi} \simeq \langle \mathbf{x} \rangle_{|\mathbf{y}, \Phi} / \sqrt{N\rho}$, indicates that the Bayesian optimal reconstruction is approximately performed as $\hat{\mathbf{x}}^{\text{Bayes}}(\mathbf{y}) \simeq \sqrt{N\rho} \mathbf{a} / |\mathbf{a}|$.

To enhance the computational tractability, let us rewrite the functional equations of (18) and (19) into algebraic equations using sets of $a_{i \rightarrow \mu}$ and $\nu_{i \rightarrow \mu}$. To do this, we insert the identity

$$\begin{aligned} 1 &= \int du_\mu \delta \left(u_\mu - \sum_{i=1}^N \Phi_{\mu i} x_i \right) \\ &= \int du_\mu \frac{1}{2\pi} \int d\hat{u}_\mu \exp \left\{ -i\hat{u}_\mu \left(u_\mu - \sum_{i=1}^N \Phi_{\mu i} x_i \right) \right\} \end{aligned} \quad (23)$$

into (18), which yields

$$\begin{aligned} m_{\mu \rightarrow i}(x_i) &= \frac{1}{2\pi Z_{\mu \rightarrow i}} \int du_\mu P(y_\mu | u_\mu) \int d\hat{u}_\mu \exp \left\{ -i\hat{u}_\mu (u_\mu - \Phi_{\mu i} x_i) \right\} \\ &\times \prod_{j \neq i} \left\{ \int dx_j m_{j \rightarrow \mu}(x_j) \exp \left\{ i\hat{u}_\mu \Phi_{\mu j} x_j \right\} \right\}. \end{aligned} \quad (24)$$

The smallness of $\Phi_{\mu i}$ allows us to truncate the Taylor series of the last exponential in equation (24) up to the second order of $i\hat{u}_\mu \Phi_{\mu j} x_j$. Integrating $\int dx_j m_{j \rightarrow \mu}(x_j) (\dots)$ for

$j \neq i$, we obtain the expression

$$m_{\mu \rightarrow i}(x_i) = \frac{1}{2\pi Z_{\mu \rightarrow i}} \int du_\mu P(y_\mu | u_\mu) \int d\hat{u}_\mu \exp \left\{ -i\hat{u}_\mu (u_\mu - \Phi_{\mu i} x_i) \right\} \\ \times \exp \left\{ i\hat{u}_\mu (\omega_\mu - \Phi_{\mu i} a_{i \rightarrow \mu}) - \frac{\hat{u}_\mu^2}{2} (V_\mu - \Phi_{\mu i}^2 \nu_{i \rightarrow \mu}) \right\}, \quad (25)$$

and carrying out the resulting Gaussian intergral of \hat{u}_μ , we obtain

$$m_{\mu \rightarrow i}(x_i) = \frac{1}{Z_{\mu \rightarrow i} \sqrt{2\pi(V_\mu - \Phi_{\mu i}^2 \nu_{i \rightarrow \mu})}} \int du_\mu P(y_\mu | u_\mu) \\ \times \exp \left\{ -\frac{(u_\mu - \omega_\mu - \Phi_{\mu i}(x_i - a_{i \rightarrow \mu}))^2}{2(V_\mu - \Phi_{\mu i}^2 \nu_{i \rightarrow \mu})} \right\}. \quad (26)$$

Since $\Phi_{\mu i}^2$ vanishes as $O(N^{-1})$ while $\nu_{i \rightarrow \mu} \sim O(1)$, we can omit $\Phi_{\mu i}^2 \nu_{i \rightarrow \mu}$ in (26). In addition, we replace $\Phi_{\mu j}^2$ in $V_\mu = \sum_i \Phi_{\mu j}^2 \nu_{i \rightarrow \mu}$ with its expectation N^{-1} , utilizing the law of large numbers. This removes the dependence on the index μ , making all V_μ equal to their average

$$V \equiv \frac{1}{N} \sum_{i=1}^N \nu_i. \quad (27)$$

The smallness of $\Phi_{\mu i}(x_i - a_{i \rightarrow \mu})$ again allows us to truncate the Taylor series of the exponential in (26) up to the second order. Thus, we have a parameterized expression of $m_{\mu \rightarrow i}(x_i)$:

$$m_{\mu \rightarrow i}(x_i) \propto \exp \left\{ -\frac{A_{\mu \rightarrow i}}{2} x_i^2 + B_{\mu \rightarrow i} x_i \right\}, \quad (28)$$

where the parameters $A_{\mu \rightarrow i}$ and $B_{\mu \rightarrow i}$ are evaluated as

$$A_{\mu \rightarrow i} = (g'_{\text{out}})_\mu \Phi_{\mu i}^2 \quad (29)$$

$$B_{\mu \rightarrow i} = (g_{\text{out}})_\mu \Phi_{\mu i} + (g'_{\text{out}})_\mu \Phi_{\mu i}^2 a_{i \rightarrow \mu} \quad (30)$$

using

$$(g_{\text{out}})_\mu \equiv \frac{\partial}{\partial \omega_\mu} \log \left(\int du_\mu P(y_\mu | u_\mu) \exp \left(-\frac{(u_\mu - \omega_\mu)^2}{2V} \right) \right) \quad (31)$$

$$(g'_{\text{out}})_\mu \equiv -\frac{\partial^2}{\partial \omega_\mu^2} \log \left(\int du_\mu P(y_\mu | u_\mu) \exp \left(-\frac{(u_\mu - \omega_\mu)^2}{2V} \right) \right). \quad (32)$$

The derivation of these is given in Appendix B. Equations (29) and (30) act as the algebraic expression of (18). In the sign output channel, inserting $P(y_\mu | u_\mu) = \Theta(u_\mu)$ into (31) gives $(g_{\text{out}})_\mu$ and $(g'_{\text{out}})_\mu$ for 1-bit CS as

$$(g_{\text{out}})_\mu = \frac{\exp \left(-\frac{\omega_\mu^2}{2V} \right)}{\sqrt{2\pi V} H \left(-\frac{\omega_\mu}{\sqrt{V}} \right)} \quad (33)$$

$$(g'_{\text{out}})_\mu = (g_{\text{out}})_\mu^2 + \frac{\omega_\mu}{V} (g_{\text{out}})_\mu. \quad (34)$$

To obtain a similar expression for (19), we substitute the last expression of (28) into (19), which leads to

$$m_{i \rightarrow \mu}(x_i) = \frac{1}{\tilde{Z}_{i \rightarrow \mu}} \left[(1 - \rho)\delta(x_i) + \rho\tilde{P}(x_i) \right] e^{-\frac{(x_i^2/2) \sum_{\gamma \neq \mu} A_{\gamma \rightarrow i} + x_i \sum_{\gamma \neq \mu} B_{\gamma \rightarrow i}}{\tilde{Z}_{i \rightarrow \mu}}}. \quad (35)$$

This indicates that $\prod_{\gamma \neq \mu} m_{\gamma \rightarrow i}(x_i)$ in (19) can be expressed as a Gaussian distribution with mean $(\sum_{\gamma \neq \mu} B_{\gamma \rightarrow i})/(\sum_{\gamma \neq \mu} A_{\gamma \rightarrow i})$ and variance $(\sum_{\gamma \neq \mu} A_{\gamma \rightarrow i})^{-1}$. Inserting these into (21) and (22) provides the algebraic expression of (19) as

$$a_{i \rightarrow \mu} = f_a \left(\frac{1}{\sum_{\gamma \neq \mu} A_{\gamma \rightarrow i}}, \frac{\sum_{\gamma \neq \mu} B_{\gamma \rightarrow i}}{\sum_{\gamma \neq \mu} A_{\gamma \rightarrow i}} \right), \quad (36)$$

$$\nu_{i \rightarrow \mu} = f_c \left(\frac{1}{\sum_{\gamma \neq \mu} A_{\gamma \rightarrow i}}, \frac{\sum_{\gamma \neq \mu} B_{\gamma \rightarrow i}}{\sum_{\gamma \neq \mu} A_{\gamma \rightarrow i}} \right), \quad (37)$$

where $f_a(\Sigma^2, R)$ and $f_c(\Sigma^2, R)$ stand for the mean and variance of an auxiliary distribution of x

$$\mathcal{M}(x|\Sigma^2, R) = \frac{1}{\mathcal{Z}(\Sigma^2, R)} \left[(1 - \rho)\delta(x) + \rho\tilde{P}(x) \right] \frac{1}{\sqrt{2\pi\Sigma^2}} e^{-\frac{(x-R)^2}{2\Sigma^2}} \quad (38)$$

where $\mathcal{Z}(\Sigma^2, R)$ is a normalization constant, respectively. For instance, when $\tilde{P}(x)$ is a Gaussian distribution of mean \bar{x} and variance σ^2 , we have

$$f_a(\Sigma^2, R) = \frac{\bar{x}\Sigma^2 + R\sigma^2}{\frac{(1-\rho)(\sigma^2+\Sigma^2)^{3/2}}{\rho\Sigma} \exp\left\{-\frac{R^2}{2\Sigma^2} + \frac{(R-\bar{x})^2}{2(\sigma^2+\Sigma^2)}\right\} + (\sigma^2 + \Sigma^2)}, \quad (39)$$

$$\begin{aligned} f_c(\Sigma^2, R) &= \left\{ \rho(1 - \rho)\Sigma (\sigma^2 + \Sigma^2)^{-5/2} \left[\sigma^2\Sigma^2 (\sigma^2 + \Sigma^2) + (\bar{x}\Sigma^2 + R\sigma^2)^2 \right] \right. \\ &\times \exp\left\{-\frac{R^2}{2\Sigma^2} - \frac{(R - \bar{x})^2}{2(\sigma^2 + \Sigma^2)}\right\} + \rho^2 \exp\left\{-\frac{(R - \bar{x})^2}{\sigma^2 + \Sigma^2}\right\} \frac{\sigma^2\Sigma^4}{(\sigma^2 + \Sigma^2)^2} \Big\} \\ &\times \left\{ (1 - \rho) \exp\left\{-\frac{R^2}{2\Sigma^2}\right\} + \rho \frac{\Sigma}{\sqrt{\sigma^2 + \Sigma^2}} \exp\left\{-\frac{(R - \bar{x})^2}{2(\sigma^2 + \Sigma^2)}\right\} \right\}^{-2}. \end{aligned} \quad (40)$$

For the signal reconstruction, we need to evaluate the moments of $m_i(x_i)$. This can be performed by simply adding back the μ dependent part to (36) and (37) as

$$a_i = f_a(\Sigma_i^2, R_i), \quad (41)$$

$$\nu_i = f_c(\Sigma_i^2, R_i), \quad (42)$$

where $\Sigma_i^2 = \left(\sum_{\mu} A_{\mu \rightarrow i}\right)^{-1}$, $R_i = \frac{\sum_{\mu} B_{\mu \rightarrow i}}{\sum_{\mu} A_{\mu \rightarrow i}}$. For large N , Σ_i^2 typically converges to a constant, independent of the index, as Σ^2 . This, in conjunction with (29) and (30), yields

$$\Sigma^2 = \left(\frac{1}{N} \sum_{\mu} (g'_{\text{out}})_{\mu} \right)^{-1}, \quad (43)$$

$$R_i = \left(\sum_{\mu} (g_{\text{out}})_{\mu} \Phi_{\mu i} \right) \Sigma^2 + a_i. \quad (44)$$

BP updates $2MN$ messages using (29), (30), (36), and (37) ($i = 1, 2, \dots, N, \mu = 1, 2, \dots, M$) in each iteration. This requires a computational cost of $O(M^2 \times N + M \times N^2)$ per iteration, which may limit the practical utility of BP to systems of relatively small size. To enhance the practical utility, let us rewrite the BP equations into those of $M+N$ messages for large N , which will result in a significant reduction of computational complexity to $O(M \times N)$ per iteration. To do this, we express $a_{i \rightarrow \mu}$ by applying Taylor's expansion to (36) around R_i as

$$\begin{aligned} a_{i \rightarrow \mu} &= f_a \left(\frac{1}{\sum_{\gamma} A_{\gamma \rightarrow i} - A_{\mu \rightarrow i}}, \frac{\sum_{\gamma} B_{\gamma \rightarrow i} - B_{\mu \rightarrow i}}{\sum_{\gamma} A_{\gamma \rightarrow i} - A_{\mu \rightarrow i}} \right) \\ &\simeq a_i + \frac{\partial f_a(\Sigma^2, R_i)}{\partial R_i} (-B_{\mu \rightarrow i} \Sigma^2) + O(N^{-1}), \end{aligned} \quad (45)$$

where $B_{\mu \rightarrow i} \sim O(N^{-1/2})$ and $\sum_{\gamma} A_{\gamma \rightarrow i} - A_{\mu \rightarrow i}$ is approximated as $\sum_{\gamma} A_{\gamma \rightarrow i} = \Sigma^{-2}$, because of the smallness of $A_{\mu \rightarrow i} \propto \Phi_{\mu i}^2 \sim O(N^{-1})$. Multiplying this by $\Phi_{\mu i}$ and summing the resultant expressions over i yields

$$\omega_{\mu} = \sum_i \Phi_{\mu i} a_i - (g_{\text{out}})_{\mu} V, \quad (46)$$

where we have used $\nu_i = f_c = \Sigma^2 \frac{\partial f_a}{\partial R_i}$, which can be confirmed by (39) and (40).

Let us assume that $\{(a_i, \nu_i)\}$ and $\{((g_{\text{out}})_{\mu}, (g'_{\text{out}})_{\mu})\}$ are initially set to certain values. Inserting these into (27) and (46) gives V and $\{\omega_{\mu}\}$. Substituting these into equations (33) and (34) yields a set of $\{((g_{\text{out}})_{\mu}, (g'_{\text{out}})_{\mu})\}$, which, in conjunction with $\{a_i\}$, offers Σ^2 and $\{R_i\}$ through (43) and (44). Inserting these into (41) and (42) offers a new set of $\{(a_i, \nu_i)\}$. In this way, the iteration of (27), (46) \rightarrow (33), (34) \rightarrow (43), (44) \rightarrow (41), (42) \rightarrow (27), (46) $\rightarrow \dots$ constitutes a closed set of equations to update the sets of $\{(a_i, \nu_i)\}$ and $\{((g_{\text{out}})_{\mu}, (g'_{\text{out}})_{\mu})\}$. This is the generic GAMP algorithm given a likelihood function $P(y|u)$ and a prior distribution $P(x)$ [13].

We term the entire procedure the Approximate Message Passing for 1-bit Compressed Sensing (1bitAMP) algorithm. The pseudocode of this algorithm is summarized in Figure 1. Three issues are noteworthy. First, for relatively large systems, e.g., $N = 1024$, the iterative procedure converges easily in most cases. Nevertheless, since it relies on the law of large numbers, some divergent behavior appears as N becomes smaller. Even for such cases, however, employing an appropriate damping factor in conjunction with a normalization of $|\mathbf{a}|$ at each update considerably improves the convergence property. Second, the most time-consuming parts of this iteration are the matrix-vector multiplications $\sum_{\mu} (g_{\text{out}})_{\mu} \Phi_{\mu i}$ in (44) and $\sum_i \Phi_{\mu i} a_i$ in (46). This indicates that the computational complexity is $O(NM)$ per iteration. Finally, a_i in equation (44) and $(g_{\text{out}})_{\mu} V$ in equation (46) correspond to what is known as the *Onsager reaction term* in the spin glass literature [20, 21]. These terms stabilize the convergence of 1bitAMP, effectively canceling the self-feedback effects.

Algorithm 1: APPROXIMATE MESSAGE PASSING FOR 1-BIT CS($\mathbf{a}^*, \nu^*, \omega^*$)

1) Initialization :

\mathbf{a} seed : $\mathbf{a}_0 \leftarrow \mathbf{a}^*$
 ν seed : $\nu_0 \leftarrow \nu^*$
 ω seed : $\omega_0 \leftarrow \omega^*$
Counter : $k \leftarrow 0$

2) Counter increase :

$k \leftarrow k + 1$

3) Mean of variances of posterior information message distributions :

$\mathbf{V}_k \leftarrow \mathbf{N}^{-1}(\text{sum}(\nu_{k-1}))\mathbf{1}$

4) Self-feedback cancellation :

$\omega_k \leftarrow \Phi \mathbf{a}_{k-1} - \mathbf{V}_k g_{\text{out}}(\omega_{k-1}, \mathbf{V}_k)$

5) Variances of output information message distributions :

$\Sigma_k^2 \leftarrow \mathbf{N}(\text{sum}(g'_{\text{out}}(\omega_k, \mathbf{V}_k)))^{-1}$

6) Average of output information message distributions :

$(\mathbf{R})_k \leftarrow \mathbf{a}_{k-1} + (g_{\text{out}}(\omega_k, \mathbf{V}_k)\Phi)\Sigma_k^2$

7) Posterior mean :

$\mathbf{a}_k \leftarrow f_a(\Sigma_k^2 \mathbf{1}, \mathbf{R}_k)$

8) Posterior variance :

$\nu_k \leftarrow f_c(\Sigma_k^2 \mathbf{1}, \mathbf{R}_k)$

9) Iteration : Repeat from step 2 until convergence.

Figure 1. Pseudocode for 1-bitAMP. \mathbf{a}^* , ν^* , and ω^* are the convergent vectors of \mathbf{a}_k , ν_k , and ω_k obtained in the previous loop. $\mathbf{1}$ is the N -dimensional vector whose entries are all unity.

5. Results

To examine the utility of 1bitAMP, we carried out numerical experiments for Gauss-Bernoulli prior,

$$P(x) = (1 - \rho) \delta(x) + \frac{\rho}{\sqrt{2\pi}} e^{-\frac{1}{2}x^2} \quad (47)$$

with system size $N = 1024$. We set initial conditions of $\mathbf{a} = 0\mathbf{1}$, $\nu = \rho\mathbf{1}$, and $\omega = \mathbf{1}$, where $\mathbf{1}$ is the N -dimensional vector whose entries are all unity, and stopped the algorithm after 20 iterations (Figure 3). The MSE results for various sets of α and ρ are shown as crosses in Figures 2 (a)–(d). Each cross denotes an experimental estimate obtained from 1000 experiments. The standard deviations are omitted, as they are smaller than the size of the symbols. The convergence time is short, which verifies the significant computational efficiency of 1bitAMP. For example, in a MATLAB[®] environment, for $\alpha = 3$, $\rho = 0.0625$, one experiment takes around 0.2 s.

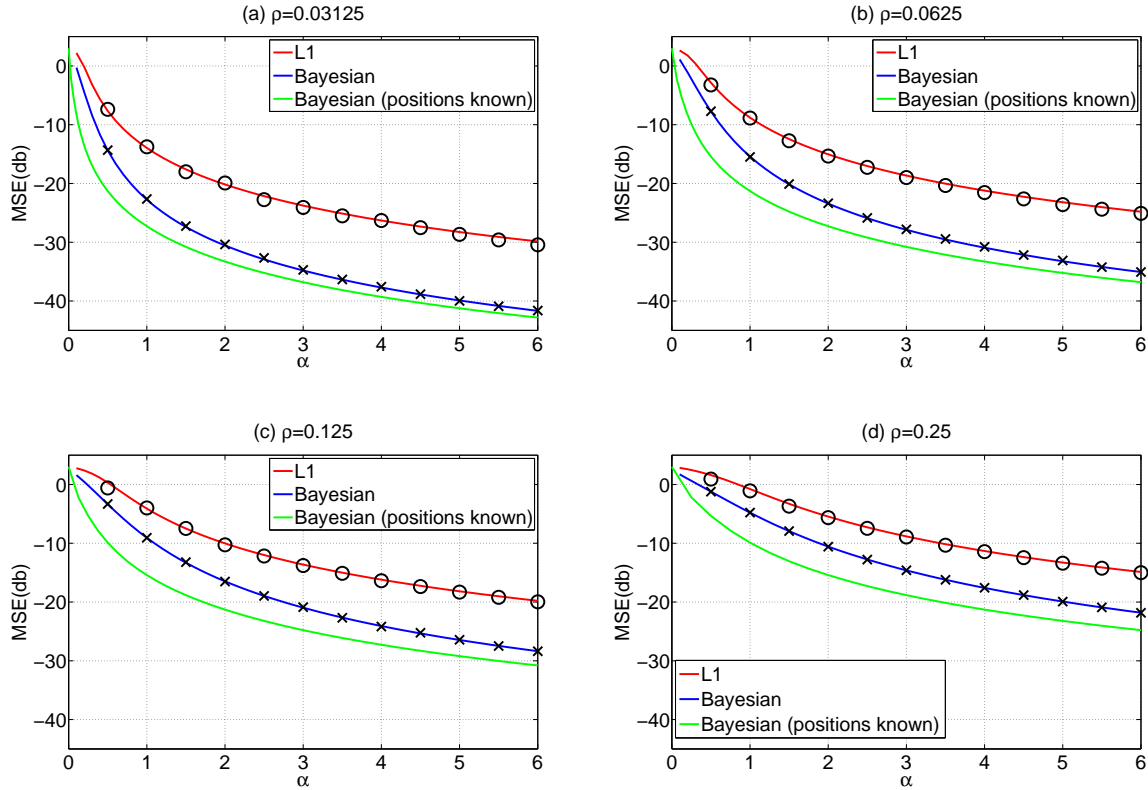


Figure 2. MSE (in decibels) versus measurement bit ratio α for 1-bit CS for Gauss-Bernoulli prior. (a), (b), (c), and (d) correspond to $\rho = 0.03125, 0.0625, 0.125$, and 0.25 , respectively. Red curves represent the theoretical prediction of l_1 -norm minimization [12]; blue curves represent the theoretical prediction of the Bayesian optimal approach; green curves represent the theoretical prediction of the Bayesian optimal approach when the positions of all nonzero components in the signal are known, which is obtained by setting $\alpha \rightarrow \alpha/\rho$ and $\rho \rightarrow 1$ in (15) and (16). Crosses represent the average of 1000 experimental results by the 1bitAMP algorithm in Figure 1 for a system size of $N = 1024$. Circles show the average of 1000 experimental results by an l_1 -based algorithm RFPI proposed in [10] for 1-bit CS in the system size of $N = 128$. Although the replica symmetric prediction for the l_1 -based approach is thermodynamically unstable, the experimental results of RFPI are numerically consistent with it very well.

To test the consistency of 1bitAMP with respect to replica theory, we solved the saddle-point equations (15) and (16) for Gauss-Bernoulli prior for each set of α and ρ . The blue curves in Figures 2 (a)–(d) show the theoretical MSE evaluated by (17) against α for $\rho = 0.03125, 0.0625, 0.125$, and 0.25 . The excellent agreement between the numerical experiments and the theoretical prediction indicates that 1bitAMP nearly saturates the potentially achievable MSE of the signal recovery scheme based on the Bayesian optimal approach.

For comparison, Figures 2 (a)–(d) also plot the replica symmetric prediction of MSEs for the l_1 -norm minimization approach (red curves) to the Gauss-Bernoulli signal,

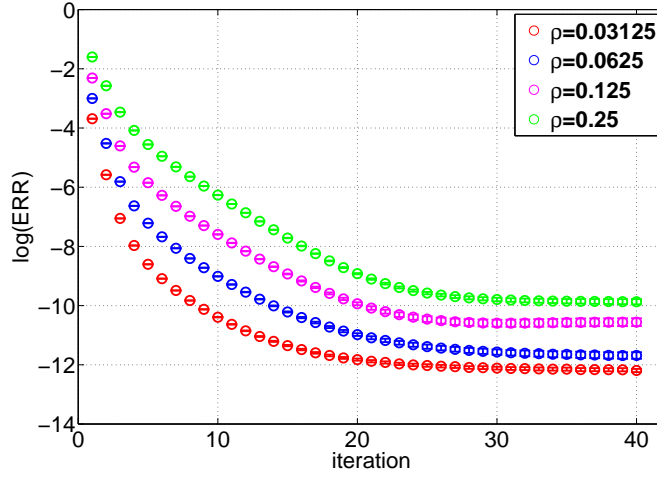


Figure 3. Mean square differences (ERR) between estimated signals of two successive iterative update of 1bitAMP for a signal size of $N = 1024$ and $\alpha = 6$, and the errorbar, which are evaluated from 10000 experiments. Red, blue, magenta, and green represent $\rho = 0.03125, 0.0625, 0.125$, and 0.25 , respectively.

which was examined in an earlier study [12]. Although the replica symmetric prediction is thermodynamically unstable, it is numerically consistent with the experimental results (circles) given by the algorithm proposed in [10]. Therefore, the prediction at least serves as a good approximation.

We also plot the MSEs of the Bayesian optimal approach when the positions of the non-zero components of \mathbf{x} are known (green curves). These act as lower bounds for the MSEs of the Bayesian optimal approach. When the positions of non-zero components of \mathbf{x} are known, we need not consider the part containing zero components. Therefore, the problem can be seen as that defined when a ρN -dimensional signal \mathbf{x} is measured by an $\alpha N \times \rho N$ -dimensional matrix. In such situations, performance can be evaluated by setting $\rho = 1$ and replacing α with α/ρ in (15) and (16), as the dimensionality of \mathbf{x} is reduced from N to $N\rho$. Solving (15) and (16) for $\alpha \gg 1$ shows that the MSEs of the Bayesian optimal approach can be asymptotically expressed as

$$\text{MSE}^{\text{Bayes}} \simeq \frac{1.9258\rho^2}{\alpha^2} = 1.9258 \times \left(\frac{N\rho}{M} \right)^2 \quad (48)$$

for $\alpha \gg 1$, which accords exactly with the asymptotic form of the green curves (Figure 4: left panel, see Appendix C). Since we defined MSE with the normalized signal, this holds for all zero mean Gauss-Bernoulli distributions of any variance. On the other hand, the asymptotic form of the MSE for the l_1 -norm approach is evaluated as

$$\text{MSE}^{l_1} \simeq \frac{\pi^2 \left[2(1 - \rho)H \left(1/\sqrt{\hat{q}_{l_1}^\infty(\rho)} \right) + \rho \right]^2}{\alpha^2}, \quad (49)$$

where $\hat{q}_{l_1}^\infty(\rho)$ is the value of \hat{q} for the l_1 -norm approach obtained for $\alpha \rightarrow \infty$ (see Appendix D).

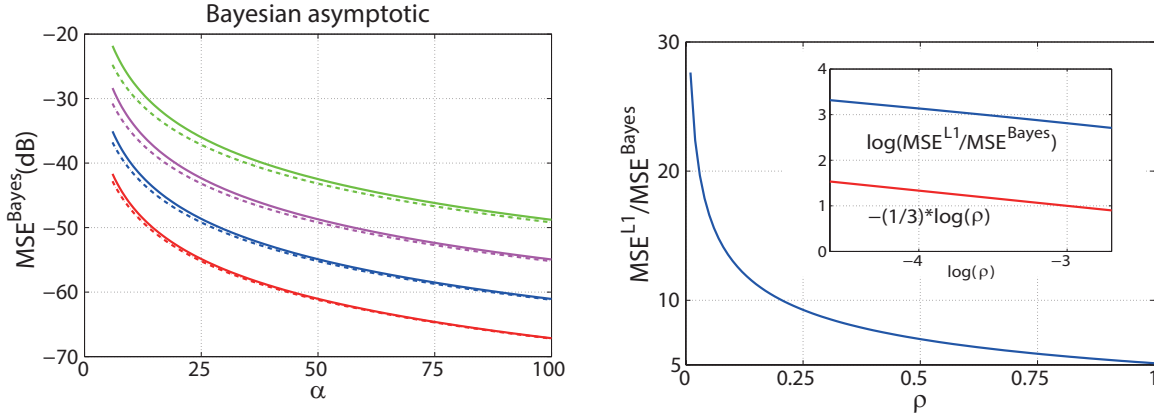


Figure 4. Left: MSE (in decibels) versus measurement bit ratio α for Bayesian optimal signal reconstruction of 1-bit CS for Gauss-Bernoulli prior. Red, blue, magenta, and green correspond to $\rho = 0.03125, 0.0625, 0.125$, and 0.25 , respectively. The solid curves represent the theoretical prediction obtained by (15) and (16); dashed curves show the performance when the positions of non-zero entries are known, and dotted curves denote the asymptotic forms (48), which are indistinguishable from the dashed curves because they closely overlap. Right: Ratio of MSE between l_1 -norm and Bayesian approaches when $\alpha \gg 1$ versus sparsity ρ of the signal. The inset shows a log-log plot for $0 < \rho < 0.1$. The least-squares fit implies that the ratio diverges as $O(\rho^{-0.33})$ as $\rho \rightarrow 0$.

Equation (48) means that, at least in terms of MSEs, correct prior knowledge of the sparsity asymptotically becomes as informative as the knowledge of the exact positions of the non-zero components. In most statistical models, the accuracy of asymptotic inference is expressed as a function of the ratio $\alpha = M/N$ between the number of data M and the dimensionality of the variables to be inferred N [22, 23]. Equation (48) indicates that, in the current problem, the dimensionality N is replaced with the actual degree of the non-zero components $N\rho$, which originates from the singularity of the prior distribution (1). This implies that caution is necessary in testing the validity of statistical models when sparse priors are employed, since conventional information criteria such as Akaike’s information criterion [24] and the minimum description length [25] mostly handle objective statistical models that are free of singularities, so that the model complexity is naively incorporated as the number of parameters N [26].

Equation (49) indicates that, even if prior knowledge of the sparsity is not available, optimal convergence can be achieved in terms of the “exponent (decay of $O(\alpha^{-2})$)” as $\alpha \rightarrow \infty$ using the l_1 -norm approach. However, the performance can differ considerably in terms of the “pre-factor (coefficient of α^{-2})”. The right panel of Figure 4 plots the ratio $\text{MSE}^{l_1} / \text{MSE}^{\text{Bayes}}$, which diverges as $O(\rho^{-0.33})$ as $\rho \rightarrow 0$. This indicates that prior knowledge of the sparsity of the objective signal is more beneficial as ρ becomes smaller.

For checking the generality of the results obtained for Gauss-Bernoulli prior, we

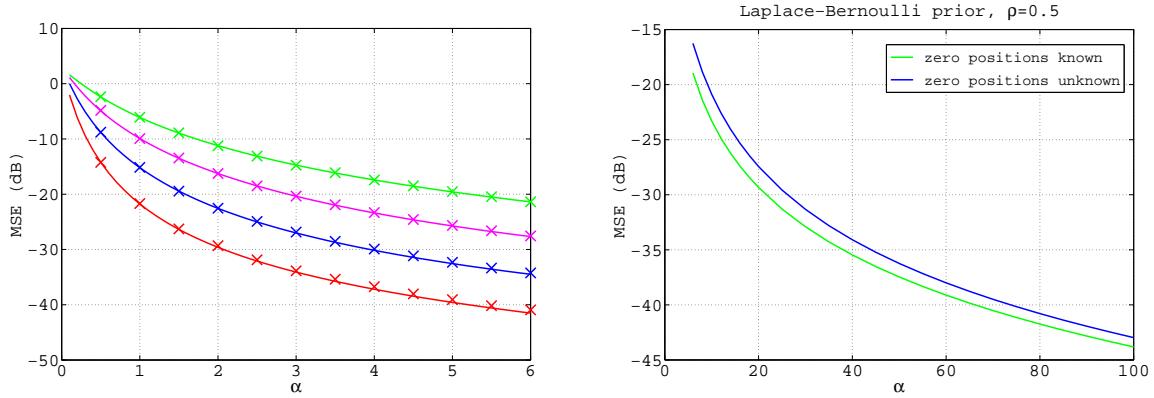


Figure 5. Left: MSE (in decibels) versus α for 1-bit CS in the case of Laplace-Bernoulli prior. Solid lines represent the theoretical prediction and the markers represent the experiment results by 1bitAMP algorithm for a signal size of $N = 1024$ and averaged from 1000 experiments. Red, blue, magenta, and green represent $\rho = 0.03125, 0.0625, 0.125$, and 0.25 , respectively. Right: Asymptotic behavior of MSE for Laplace-Bernoulli prior, when the positions of zero entries of the signal are known and unknown. This implies that MSE of these two cases are different even asymptotically.

also carried out similar analysis for Laplace-Bernoulli prior

$$P(x) = (1 - \rho) \delta(x) + \frac{\rho}{2} e^{-|x|}. \quad (50)$$

The left panel of Fig. 5 shows the comparison between the replica prediction and the experimental results by GAMP, which supports that the replica and GAMP correspondence does hold for general priors. The right panel of Fig. 5 compares the performance with that achieved when the positions of non-zero entries are known. Unlike the case of Gauss-Bernoulli prior, the two performances do not get close even asymptotically. This implies that the significance of utility of the Bayesian approach depends considerably on the statistical property of the objective signal.

6. Summary

In summary, we have examined the typical performance of the Bayesian optimal signal recovery for 1-bit CS using methods from statistical mechanics. For Gauss-Bernoulli prior, using the replica method to compare the performance of the Bayesian optimal approach to the l_1 -norm minimization, we have shown that the utility of correct prior knowledge on the objective signal, which is incorporated in the Bayesian optimal scheme, becomes more significant as the density of non-zero entries ρ in the signal decreases. In addition, we have clarified that, for this particular prior, the MSE performance asymptotically saturates that obtained when the exact positions of non-zero entries are exactly known as the number of 1-bit measurements increases. We have also

developed a practically feasible approximate algorithm for Bayesian signal recovery, which can be regarded as a special case of the GAMP algorithm. The algorithm has a computational cost of the square of the system size per update, exhibiting a fairly good convergence property as the system size becomes larger. The experimental results for both Gauss-Bernoulli prior and Laplace-Bernoulli prior show excellent agreement with the predictions made by the replica method. These indicate that almost-optimal reconstruction performance can be attained with a computational complexity of the square of the signal length per update for general priors, which is highly beneficial in practice.

Obtaining the correct prior distribution of the sparse signal may be an obstacle to applying the current approach in practical problems. One possible solution is to estimate hyper-parameters that characterize the prior distribution in the reconstruction stage, as has been proposed for normal CS [9]. It was reported that orthogonal measurement matrices, rather than those of statistically independent entries, enhance the signal reconstruction performance for several problems related to CS [32, 33, 34, 35, 36, 37]. Such devices may also be effective for 1-bit CS.

Acknowledgments

YX is supported by JSPS Research Fellowships DC2. This study was also partially supported by the JSPS Core-to-Core Program “Non-equilibrium dynamics of soft matter and information,” JSPS KAKENHI Nos. 26011287 (YX), 25120013 (YK), and the Grant DySpaN of Triangle de la Physique (LZ). Useful discussions with Chistophe Schülke are also acknowledged.

Appendix A. Derivation of (13)

Appendix A.1. Assessment of $[P^n(\mathbf{y}|\Phi)]_{\Phi, \mathbf{y}}$ for $n \in \mathbb{N}$

Averaging (10) with respect to Φ and \mathbf{y} gives the following expression for the n -th moment of the partition function:

$$[P^n(\mathbf{y}|\Phi)]_{\Phi, \mathbf{y}} = \int \prod_{a=1}^n (d\mathbf{x}^a P(\mathbf{x}^a)) \times \left[\prod_{a=1}^n \prod_{\mu=1}^M \Theta((\mathbf{y})_{\mu}(\Phi \mathbf{x}^a)_{\mu}) \right]_{\Phi, \mathbf{y}}. \quad (\text{A.1})$$

We insert $n(n+1)/2$ trivial identities

$$1 = N \int dq_{ab} \delta(\mathbf{x}^a \cdot \mathbf{x}^b - Nq_{ab}), \quad (\text{A.2})$$

where $a > b = 0, 1, 2, \dots, n$, into (A.1). Furthermore, we define a joint distribution of $n+1$ vectors $\{\mathbf{x}^a\} = \{\mathbf{x}^0, \mathbf{x}^1, \mathbf{x}^2, \dots, \mathbf{x}^n\}$ as

$$P(\{\mathbf{x}^a\}|\mathbf{Q}) = \frac{1}{V(\mathbf{Q})} P(\mathbf{x}^0) \times \prod_{a=1}^n (P(\mathbf{x}^a)) \times \prod_{a>b} \delta(\mathbf{x}^a \cdot \mathbf{x}^b - Nq_{ab}), \quad (\text{A.3})$$

where $\mathbf{Q} = (q_{ab})$ is an $(n+1) \times (n+1)$ symmetric matrix whose 00 and other diagonal entries are fixed as ρ and Q , respectively. $P(\mathbf{x}^0) = \prod_{i=1}^N \left((1-\rho)\delta(x_i^0) + \rho\tilde{P}(x_i^0) \right)$ denotes the distribution of the original signal \mathbf{x}^0 , and $V(\mathbf{Q})$ is the normalization constant that ensures $\int \prod_{a=0}^n d\mathbf{x}^a P(\{\mathbf{x}^a\}|\mathbf{Q}) = 1$ holds. These indicate that (A.1) can also be expressed as

$$[P^n(\mathbf{y}|\Phi)]_{\Phi, \mathbf{y}} = \int d\mathbf{Q} (V(\mathbf{Q}) \times \Xi(\mathbf{Q})), \quad (\text{A.4})$$

where $d\mathbf{Q} \equiv \prod_{a>b} dq_{ab}$ and

$$\Xi(\mathbf{Q}) = \int \prod_{a=0}^n d\mathbf{x}^a P(\{\mathbf{x}^a\}|\mathbf{Q}) \left[\sum_{\mathbf{y}} \prod_{a=0}^n \prod_{\mu=1}^M \Theta(((\mathbf{y})_{\mu}(\Phi \mathbf{x}^a)_{\mu})) \right]_{\Phi}. \quad (\text{A.5})$$

Equation (A.5) can be regarded as the average of $\sum_{\mathbf{y}} \prod_{a=0}^n \prod_{\mu=1}^M \Theta(((\mathbf{y})_{\mu}(\Phi \mathbf{x}^a)_{\mu}))$ with respect to $\{\mathbf{x}^a\}$ and Φ over distributions of $P(\{\mathbf{x}^a\})$ and $P(\Phi) \equiv \left(\sqrt{2\pi/N} \right)^{-MN} \exp \left(-(N/2) \sum_{\mu,i} \Phi_{\mu i}^2 \right)$. In computing this, note that the central limit theorem guarantees that $u_{\mu}^a \equiv (\Phi \mathbf{x}^a)_{\mu} = \sum_{i=1}^N \Phi_{\mu i} x_i^a$ can be handled as zero-mean multivariate Gaussian random numbers whose variance and covariance are given by

$$[u_{\mu}^a u_{\nu}^b]_{\Phi, \{\mathbf{x}^a\}} = \delta_{\mu\nu} q_{ab}, \quad (\text{A.6})$$

when Φ and $\{\mathbf{x}^a\}$ are generated independently from $P(\Phi)$ and $P(\{\mathbf{x}^a\})$, respectively. This means that (A.5) can be evaluated as

$$\begin{aligned} \Xi(\mathbf{Q}) &= \left(\frac{\int d\mathbf{u} \exp \left(-\frac{1}{2} \mathbf{u}^T \mathbf{Q}^{-1} \mathbf{u} \right) \sum_{\mathbf{y} \in \{+1, -1\}} \prod_{a=0}^n \Theta(\mathbf{y} \mathbf{u}^a)}{(2\pi)^{(n+1)/2} (\det \mathbf{Q})^{1/2}} \right)^M \\ &= \left(2 \int \frac{d\mathbf{u} \exp \left(-\frac{1}{2} \mathbf{u}^T \mathbf{Q}^{-1} \mathbf{u} \right) \prod_{a=0}^n \Theta(\mathbf{u}^a)}{(2\pi)^{(n+1)/2} (\det \mathbf{Q})^{1/2}} \right)^M. \end{aligned} \quad (\text{A.7})$$

On the other hand, expressions

$$\delta(|\mathbf{x}^a|^2 - NQ) = \frac{1}{4\pi} \int_{-\infty}^{+\infty} d\hat{q}_{aa} \exp \left(-\frac{1}{2} \hat{q}_{aa} (|\mathbf{x}^a|^2 - NQ) \right) \quad (\text{A.8})$$

and

$$\delta(\mathbf{x}^a \cdot \mathbf{x}^b - Nq_{ab}) = \frac{1}{2\pi} \int_{-\infty}^{+\infty} d\hat{q}_{ab} \exp \left(\hat{q}_{ab} (\mathbf{x}^a \cdot \mathbf{x}^b - Nq_{ab}) \right), \quad (\text{A.9})$$

and use of the saddle-point method, offer

$$\begin{aligned} \frac{1}{N} \log V(\mathbf{Q}) &= \text{extr}_{\hat{\mathbf{Q}}} \left\{ -\frac{1}{2} \text{Tr} \hat{\mathbf{Q}} \mathbf{Q} \right. \\ &\quad \left. + \log \left(\int d\mathbf{x} P(\mathbf{x}^0) \prod_{a=1}^n P(\mathbf{x}^a) \exp \left(\frac{1}{2} \mathbf{x}^T \hat{\mathbf{Q}} \mathbf{x} \right) \right) \right\}. \end{aligned} \quad (\text{A.10})$$

Here, $\mathbf{x} = (x^0, x^1, \dots, x^n)^T$ and $\hat{\mathbf{Q}}$ is an $(n+1) \times (n+1)$ symmetric matrix whose 00 and other diagonal components are given as 0 and $-\hat{q}_{aa}$, respectively. The off-diagonal entries are \hat{q}_{ab} . Equations (A.7) and (A.10) indicate that $N^{-1} \log [P^n(\mathbf{y}|\Phi)]_{\Phi, \mathbf{y}}$ is correctly evaluated by the saddle-point method with respect to \mathbf{Q} in the assessment of the right-hand side of (A.4), when N and M tend to infinity and $\alpha = M/N$ remains finite.

Appendix A.2. Treatment under the replica symmetric ansatz

Let us assume that the relevant saddle-point for assessing (A.4) is of the form (12) and, accordingly,

$$\hat{q}_{ab} = \hat{q}_{ba} = \begin{cases} 0, & (a = b = 0) \\ \hat{m}, & (a = 1, 2, \dots, n; b = 0) \\ \hat{Q}, & (a = b = 1, 2, \dots, n) \\ \hat{q}, & (a \neq b = 1, 2, \dots, n) \end{cases}. \quad (\text{A.11})$$

The $n+1$ -dimensional Gaussian random variables u^0, u^1, \dots, u^n whose variance and covariance are given by (12) can be expressed as

$$u^0 = \sqrt{\rho - \frac{m^2}{q}} s^0 + \frac{m}{\sqrt{q}} z, \quad (\text{A.12})$$

$$u^a = \sqrt{Q - q} s^a + \sqrt{q} z, \quad (a = 1, 2, \dots, n) \quad (\text{A.13})$$

utilizing $n+2$ independent standard Gaussian random variables z and s^0, s^1, \dots, s^n . This indicates that (A.7) is evaluated as

$$\Xi(\mathbf{Q}) = \left(2 \int \text{D}z H \left(\frac{m}{\sqrt{\rho q - m^2}} z \right) H^n \left(\sqrt{\frac{q}{Q - q}} z \right) \right)^M. \quad (\text{A.14})$$

On the other hand, substituting (A.11) into (A.10), in conjunction with the identity

$$\exp \left(\hat{q} \sum_{a>b(\geq 1)} x^a x^b \right) = \int \text{D}z \exp \left(\sum_{a=1}^n \left(-\frac{\hat{q}}{2} (x^a)^2 + \sqrt{\hat{q}} z x^a \right) \right), \quad (\text{A.15})$$

provides

$$\begin{aligned} \frac{1}{N} \log V(\mathbf{Q}) = & \text{extr}_{\hat{Q}, \hat{q}, \hat{m}} \left\{ \frac{n}{2} \hat{Q} Q - \frac{n(n-1)}{2} \hat{q} q - \hat{m} m \right. \\ & \left. + \log \left[\left(\int dx P(x) \exp \left(-\frac{\hat{Q} + \hat{q}}{2} x^2 + (\sqrt{\hat{q}} z + \hat{m} x^0) x \right) \right)^n \right]_{x^0, z} \right\}. \end{aligned} \quad (\text{A.16})$$

Although we have assumed that $n \in \mathbb{N}$, the expressions of (A.14) and (A.16) are likely to hold for $n \in \mathbb{R}$ as well. Therefore, the average free energy \bar{f} can be evaluated by substituting these expressions into the formula $\bar{f} = \lim_{n \rightarrow 0} (\partial / \partial n) \left((N)^{-1} \log [P^n(\mathbf{y}|\Phi)]_{\Phi, \mathbf{y}} \right)$.

Furthermore, employing the expressions that hold for $|n| \ll 1$, $H^n(x) = \exp(n \log H(x)) \approx 1 + n \log H(x)$ and $\log(1 + nC(\cdot)) \approx nC(\cdot)$, where $C(\cdot)$ is an arbitrary function, we obtain the form

$$\lim_{n \rightarrow 0} \frac{\partial}{\partial n} \frac{1}{N} \log \Xi(\mathbf{Q}) = 2\alpha \int \mathrm{D}z H\left(\frac{m}{\sqrt{\rho q - m^2}}z\right) \log H\left(\sqrt{\frac{q}{Q - q}}z\right). \quad (\text{A.17})$$

And we have

$$\begin{aligned} \lim_{n \rightarrow 0} \frac{\partial}{\partial n} \frac{1}{N} \log V(\mathbf{Q}) = & \underset{\hat{Q}, \hat{q}, \hat{m}}{\text{extr}} \left\{ \int \mathrm{d}x^0 P(x^0) \int \mathrm{D}z \phi\left(\sqrt{\hat{q}}z + \hat{m}x^0; \hat{Q}\right) \right. \\ & \left. + \frac{1}{2}Q\hat{Q} + \frac{1}{2}q\hat{q} - m\hat{m} \right\}. \end{aligned} \quad (\text{A.18})$$

Using these in the resultant expression of \bar{f} gives (13).

Appendix B. Derivation of (28)–(32)

Expanding the exponential in (26) up to the second order of $\Phi_{\mu i}(x_i - a_{i \rightarrow \mu})$ and performing the integration with respect to u_μ gives

$$\begin{aligned} m_{\mu \rightarrow i}(x_i) & \simeq c_0 + c_1 \Phi_{\mu i}(x_i - a_{i \rightarrow \mu}) + \frac{1}{2} c_2 \Phi_{\mu i}^2(x_i - a_{i \rightarrow \mu})^2 \\ & \simeq \exp \left\{ \ln c_0 + \frac{c_1}{c_0} \Phi_{\mu i}(x_i - a_{i \rightarrow \mu}) + \frac{c_0 c_2 - c_1^2}{2c_0^2} \Phi_{\mu i}^2(x_i - a_{i \rightarrow \mu})^2 \right\} \\ & \propto \exp \left\{ -\frac{A_{\mu \rightarrow i}}{2} x_i^2 + B_{\mu \rightarrow i} x_i \right\}, \end{aligned} \quad (\text{B.1})$$

where

$$c_0 \equiv \int \mathrm{d}u_\mu P(y_\mu | u_\mu) \exp \left(-\frac{(u_\mu - \omega_\mu)^2}{2V} \right), \quad (\text{B.2})$$

$$c_1 \equiv \int \mathrm{d}u_\mu P(y_\mu | u_\mu) \left(\frac{u_\mu - \omega_\mu}{V} \right) \exp \left(-\frac{(u_\mu - \omega_\mu)^2}{2V} \right), \quad (\text{B.3})$$

$$c_2 \equiv \int \mathrm{d}u_\mu P(y_\mu | u_\mu) \left(\left(\frac{u_\mu - \omega_\mu}{V} \right)^2 - \frac{1}{V} \right) \exp \left(-\frac{(u_\mu - \omega_\mu)^2}{2V} \right), \quad (\text{B.4})$$

and

$$A_{\mu \rightarrow i} = \frac{c_1^2 - c_0 c_2}{c_0^2} \Phi_{\mu i}^2, \quad (\text{B.5})$$

$$B_{\mu \rightarrow i} = \frac{c_1}{c_0} \Phi_{\mu i} + \frac{c_1^2 - c_0 c_2}{c_0^2} \Phi_{\mu i}^2 a_{i \rightarrow \mu}. \quad (\text{B.6})$$

Equations (B.3) and (B.4) imply that c_1 and c_2 can be expressed as $c_1 = \partial c_0 / \partial \omega_\mu$ and $c_2 = \partial^2 c_0 / \partial \omega_\mu^2$, respectively. Inserting this into (B.5) and (B.6), we obtain (28)–(32).

Appendix C. Asymptotic form of $\text{MSE}^{\text{Bayes}}$

The behavior as $m \rightarrow \rho$ and $\hat{m} \rightarrow \infty$ is obtained as $\alpha \rightarrow \infty$. This implies that, for Gauss-Bernoulli distribution, equations (15) and (16) can be evaluated as

$$\begin{aligned} m &= \int \text{D}t \frac{\rho^2(1+\hat{m})^{-1} e^{\frac{\hat{m}}{1+\hat{m}}t^2} \frac{\hat{m}}{(1+\hat{m})^2} t^2}{1-\rho+\rho(1+\hat{m})^{-1/2} e^{\frac{\hat{m}}{2(1+\hat{m})}t^2}} \\ &= \frac{\rho^2 \hat{m}}{(1+\hat{m})} \int \text{D}z z^2 \left[(1-\rho)(1+\hat{m})^{1/2} e^{-\frac{\hat{m}}{2}z^2} + \rho \right]^{-1} \\ &\simeq \rho(1-\hat{m}^{-1}) \end{aligned} \quad (\text{C.1})$$

and

$$\begin{aligned} \hat{m} &= \frac{2\alpha}{\rho-m} \int \text{D}t \frac{e^{-\frac{m}{\rho-m}t^2}/(2\pi)}{H\left(\sqrt{\frac{m}{\rho-m}}t\right)} = \frac{2\alpha}{\sqrt{m(\rho-m)}} \int \frac{\text{d}z}{(2\pi)^{3/2}} \frac{e^{-\frac{\rho+m}{2m}z^2}}{H(z)} \\ &\simeq \frac{2C\alpha}{\sqrt{m(\rho-m)}}, \end{aligned} \quad (\text{C.2})$$

respectively. Here, the integration variables have been changed to $(1+\hat{m})^{-1/2}t = z$ and $\sqrt{m/(\rho-m)}t = z$ in (C.1) and (C.2), respectively, and we set $C \equiv \int \text{d}z (2\pi)^{-3/2} e^{-z^2}/H(z) = 0.3603\dots$. Equations (C.1) and (C.2) yield an asymptotic expression for m :

$$m \simeq \rho \left(1 - \left(\frac{\rho}{2C\alpha} \right)^2 \right). \quad (\text{C.3})$$

Inserting this into (17) gives (48).

The performance when the positions of non-zero entries are known can be evaluated by setting $\rho = 1$ and replacing α with α/ρ in (15) and (16) as the dimensionality of \mathbf{x} is reduced from N to $N\rho$. This reproduces (48) in the asymptotic region of $\alpha \gg 1$.

Appendix D. Asymptotic form of MSE^{l_1}

The saddle-point equations of the l_1 -norm minimization approach under a normalization constraint of $|\mathbf{x}|^2 = N$ are as follows [12]:

$$\hat{q} = \frac{\alpha}{\pi\chi^2} \left(\arctan\left(\frac{\sqrt{\rho-m^2}}{m}\right) - \frac{m}{\rho} \sqrt{\rho-m^2} \right), \quad (\text{D.1})$$

$$\hat{m} = \frac{\alpha}{\pi\chi\rho} \sqrt{\rho-m^2}, \quad (\text{D.2})$$

$$\begin{aligned} \hat{Q}^2 = 2 \left\{ (1-\rho) \left[(\hat{q}+1) H\left(\frac{1}{\sqrt{\hat{q}}}\right) - \sqrt{\frac{\hat{q}}{2\pi}} e^{-\frac{1}{2\hat{q}}} \right] \right. \\ \left. + \rho \left[(\hat{q} + \hat{m}^2 + 1) H\left(\frac{1}{\sqrt{\hat{q} + \hat{m}^2}}\right) - \sqrt{\frac{\hat{q} + \hat{m}^2}{2\pi}} e^{-\frac{1}{2(\hat{q} + \hat{m}^2)}} \right] \right\}, \end{aligned} \quad (\text{D.3})$$

$$\chi = \frac{2}{\hat{Q}} \left[(1-\rho) H\left(\frac{1}{\sqrt{\hat{q}}}\right) + \rho H\left(\frac{1}{\sqrt{\hat{q} + \hat{m}^2}}\right) \right], \quad (\text{D.4})$$

$$m = \frac{2\rho\hat{m}}{\hat{Q}} H\left(\frac{1}{\sqrt{\hat{q} + \hat{m}^2}}\right). \quad (\text{D.5})$$

The behavior as $m \rightarrow \sqrt{\rho}$ and $\hat{m} \rightarrow \infty$ is obtained as $\alpha \rightarrow \infty$. This implies that (D.3) can be evaluated as

$$\begin{aligned} \hat{Q} &\simeq \left(\rho\hat{m}^2 - \frac{4\hat{m}}{\sqrt{2\pi}} + B(\hat{q}, \rho) \right)^{1/2} \\ &\simeq \sqrt{\rho}\hat{m} \left[1 - \frac{2}{\sqrt{2\pi}\hat{m}} + \left(\frac{B(\hat{q}, \rho)}{2\rho} - \frac{3}{\pi} \right) \right], \end{aligned} \quad (\text{D.6})$$

where $B(\hat{q}, \rho) \equiv \rho(\hat{q}+1) + 2(1-\rho) \left[(\hat{q}+1) H\left(\frac{1}{\sqrt{\hat{q}}}\right) - \sqrt{\frac{\hat{q}}{2\pi}} e^{-\frac{1}{2\hat{q}}} \right]$. Inserting (D.6) into (D.5), we obtain

$$m \simeq \sqrt{\rho}(1-\delta), \quad (\text{D.7})$$

where

$$\delta \equiv \left(\frac{B(\hat{q}, \rho)}{2\rho} - \frac{1}{\pi} \right) / \hat{m}^2 = \pi^2 \left[2(1-\rho) H\left(1/\sqrt{\hat{q}}\right) + \rho \right]^2 / (2\alpha^2). \quad (\text{D.8})$$

Inserting (D.2), (D.6), (D.7), and $\chi \simeq [2(1-\rho)H(1/\sqrt{\hat{q}})]/\hat{Q}$ into (D.1) yields a closed equation with respect to \hat{q} :

$$\hat{q} \simeq \frac{2}{3} \left(B(\hat{q}, \rho) - \frac{2\rho}{\pi} \right) \left[2(1-\rho)H(1/\sqrt{\hat{q}}) + \rho \right]^{-1}. \quad (\text{D.9})$$

This determines the value of \hat{q} for $\alpha \rightarrow \infty$, $\hat{q}_{l_1}^\infty(\rho)$. Combining (D.8) and

$$\text{MSE}^{l_1} = 2 \left(1 - \frac{m}{\sqrt{\rho}} \right) \simeq 2\delta \quad (\text{D.10})$$

gives (49) in the asymptotic region of $\alpha \gg 1$.

References

- [1] <https://sites.google.com/site/igorcarron2/compressedsensingshardware>
- [2] Elad M, 2010 *Sparse and Redundant Representations: From Theory to Applications in Signal and Image Processing* (New York: Springer)
- [3] Starck J-L, Murtagh F and Fadili J M, 2010 *Sparse Image and Signal Processing: Wavelets, Curvelets, Morphological Diversity* (New York: Cambridge University Press)
- [4] Candès E J and Wakin M B, 2008 *IEEE Signal Processing Magazine* March 2008, 21
- [5] Donoho D L, 2006 *IEEE Trans. Inform. Theory* **52** 1289
- [6] Candès E J, Romberg J and Tao T, 2006 *IEEE Trans. Inform. Theory* **52** 489
- [7] Kabashima Y, Wadayama T and Tanaka T, *J. Stat. Mech.* (2009) L09003; *J. Stat. Mech.* (2012) E07001
- [8] Ganguli S and Sompolinsky H, 2010 *Phys. Rev. Lett.* **104** 188701
- [9] Krzakala F, Mézard M, Sausset F, Sun Y F and Zdeborová L, 2012 *Phys. Rev. X* **2** 021005
- [10] Boufounos P T and Baraniuk R G 2008 in *Proceedings of CISS2008* 16
- [11] Lee D, Sasaki T, Yamada T, Akabane K, Yamaguchi Y and Uehara K, 2012 in *Proceedings of IEEE Vehicular Technology Conference (VTC Spring)*
- [12] Xu Y and Kabashima Y, 2013 *J. Stat. Mech.* P02041
- [13] Rangan, S. *Generalized approximate message passing for estimation with random linear mixing*, Information Theory Proceedings (ISIT), 2011 IEEE International Symposium on; arXiv: 1010.5141v1 [cs.IT], 2010
- [14] Kabashima Y and Uda S, 2004 *A BP-based algorithm for performing Bayesian inference in large perceptron-type networks*, S. Ben-David, J. Case, and Maruoka (eds.), ALT 2004, Lecture Notes in AI, Springer, vol.3244, pp.479-493.
- [15] Dotsenko V S, 2001 *Introduction to the Replica Theory of Disordered Statistical Systems*, (Cambridge: Cambridge University Press)
- [16] Nishimori H, 2001 *Statistical Physics of Spin Glasses and Information Processing*, (Oxford: Oxford University Press)
- [17] H. Nishimori and D. Sherrington, *Absence of Replica Symmetry Breaking in a Region of the Phase Diagram of the Ising Spin Glass*, in “Disordered and Complex Systems”, Ed. P. Sollich et al, AIP Conf. Proc. 553, p. 67 (2001)
- [18] A. Montanari, *Estimating Random Variables from Random Sparse Observations*, European Transactions on Telecommunications 19, 385403 (2008)
- [19] Donoho D L, Maleki A and Montanari A, 2009 *Message-passing algorithms for compressed sensing*, Proc. Nat. Acad. Sci. 106 18914
- [20] Thouless D J, Anderson P W and Palmer R G, 1977 *Phil. Mag.* **35** 593
- [21] Shiino M and Fukai T, 1992 *J. Phys. A* **25** L375
- [22] Seung H S, Sompolinsky H and Tishby N, 1992 *Phys. Rev. A* **45** 6056
- [23] Watkin T L H, Rau A and Biehl M, 1993 *Rev. Mod. Phys.* **65** 499
- [24] Akaike H, 1974 *IEEE Trans. on AC* **19** 716
- [25] Rissanen J, 1978 *Automatica* **14** 465
- [26] Watanabe S, 2009 *Algebraic Geometry and Statistical Learning Theory* (Cambridge University Press, Cambridge, UK)
- [27] Mézard M, Parisi G and Virasoro M A, 1987 *Spin Glass Theory and Beyond* (Singapore: World Scientific)
- [28] Mézard M and Montanari M, 2009 *Information, Physics, and Computation*(New York: Oxford University Press)
- [29] MacKay D J C, 1999 *IEEE Trans. Inform. Theory* **45** 399; MacKay D J C and Neal R M, 1997 *Elect. Lett.* **33** 457
- [30] Kabashima Y and Saad D, 1998 *Europhys. Lett.* **44** 668
- [31] de Almeida J R L and Thouless D J, 1978 *J. Phys. A* **11** 983

- [32] Shizato T and Kabashima Y, 2009 *J. Phys. A* **42** 015005
- [33] Kabashima Y, Vehkaperä M and Chatterjee S, 2012 *J. Stat. Mech.* P12003
- [34] Vehkaperä M, Kabashima Y and Chatterjee S, 2013 *Analysis of Regularized LS Reconstruction and Random Matrix Ensembles in Compressed Sensing*, arXiv:1312.0256
- [35] Kabashima Y and Vehkaperä M, 2014 *Signal recovery using expectation consistent approximation for linear observations*, arXiv:1401.5151
- [36] Oymak S and Hassibi B, 2014 *A Case for Orthogonal Measurements in Linear Inverse Problems*, Preprint <http://www.its.caltech.edu/~soymak/OHUnitary.pdf>
- [37] Wen C-K and Wong K-K, 2014 *Analysis of Compressed Sensing with Spatially-Coupled Orthogonal Matrices*, arXiv:1402.3215